The Canadian Mineralogist
Vol. 34, pp. 1149-1162 (1996)

INFLUENCE OF MAGMATIC ASSIMILATION ON MINERAL GROWTH AND ZONING

BENJAMIN R. EDWARDS AND JAMES K. RUSSELL[1]

Department of Earth and Ocean Sciences, University of British Columbia, 6339 Stores Road, Vancouver, British Columbia V6T 1Z4

ABSTRACT

We explore the potential effects of magmatic assimilation on mineral growth and mineral zoning in an alkali olivine basaltic magma using both equilibrium thermodynamics and kinetics. The equilibrium-model calculations simulate fractional crystallization alone (closed system) and coupled assimilation – fractional crystallization (AFC) (open system); the models predict the assemblages of magmatic minerals expected and the ranges of mineral compositions. The AFC simulations are varied to show the consequences of bulk assimilation of granite *versus* the selective assimilation of minerals of the same granite. The resulting paths are strongly affected by the nature and type of assimilation; differences between the paths are reflected in the predicted patterns of compositional zoning in feldspar and pyroxene. These results strongly support the concept of using patterns of mineral zoning a) to identify open-system behavior, b) to restrict the identity or nature of the assimilant, and c) to constrain the extent of assimilation. In particular, these results could provide important constraints in determinations of ratios of assimilation to crystallization in the context of trace-element and isotopic studies of AFC. Mineral zoning may also help to identify the specific mechanisms that control how xenoliths react with their host magmas, since kinetic models indicate that in most cases, magmatic assimilation operates selectively. Integration of kinetic constraints with current thermodynamic models of magmatic phase-equilibria should ultimately produce accurate chemical models of magmatic assimilation and a greater understanding of mineral-zoning patterns.

Keywords: magmatic assimilation, mineral zoning, equilibrium thermodynamic modeling, kinetics, feldspar, pyroxene.

SOMMAIRE

Nous explorons ici les effets potentiels de l'assimilation magmatique sur la croissance cristalline et sur la zonation des minéraux dans un magma basaltique à tendance alcaline, cristallisant de l'olivine, en utilisant comme outils la thermodynamique pour systèmes à l'équilibre et la cinétique. Les calculs fondés sur le modèle d'équilibre simulent la cristallisation fractionnée seule (système fermé) ou bien la situation de cristallisation fractionnée couplée à l'assimilation (AFC; système ouvert). Les modèles prédisent les assemblages de minéraux magmatiques attendus et leurs intervalles de composition. On varie les schémas de AFC afin de montrer les conséquences de l'assimilation massive de granite d'une part, et l'assimilation sélective des minéraux du même granite de l'autre. Les tracés qui en résultent dépendent fortement de la nature et du type d'assimilation. Les différences se voient dans la zonation du feldspath et du pyroxène. Ces résultats viennent renforcer l'utilisation des schémas de zonation pour a) identifier un comportement en système ouvert, b) cerner l'identité ou la nature de l'assimilant, et c) placer des limites sur la portée de l'assimilation. En particulier, ces résultats pourraient bien placer des limites importantes dans la détermination des rapports du degré d'assimilation au degré de cristallisation dans le contexte d'études des phénomènes AFC utilisant les éléments traces et les systèmes isotopiques. Le tracé de zonation des minéraux serait aussi utile pour identifier les mécanismes précis qui régissent le comportement des xénolithes en présence d'un magma hôte; les modèles cinétiques montrent que dans la plupart des cas, l'assimilation magmatique procède sélectivement. L'intégration des restrictions cinétiques et des modèles thermodynamiques courants de l'équilibre des phases dans les systèmes magmatiques devrait éventuellement produire des modèles chimiques justes de l'assimilation magmatique et de la zonation chimique dans les minéraux produits.

(Traduit par la Rédaction)

Mots-clés: assimilation magmatique, zonation des minéraux, modèle thermodynamique à l'équilibre, cinétique, feldspath, pyroxène.

[1]*E-mail address:* russell@earth.eos.ubc.ca

INTRODUCTION

Compositional zoning in magmatic minerals can retain a record of the physicochemical conditions extant during crystallization (Pringle *et al.* 1974, Sibley *et al.* 1976, Kuo & Kirkpatrick 1982, Anderson 1984, Pearce 1994, Nekvasil 1994). Patterns of growth of magmatic minerals can be used effectively to: a) record changes in the magmatic environment (Wiebe 1968, Pringle *et al.* 1974, Uebel 1978, Kuo & Kirkpatrick 1982, Pearce *et al.* 1987a, b), b) constrain histories and mechanisms of crystallization (Sibley *et al.* 1976, Nixon & Pearce 1987, Russell *et al.* 1987), and c) constrain the dynamics of open systems (Nixon & Pearce 1987, Jamtveit 1991). Most importantly, in the context of this study, both compositional zoning and growth features in magmatic minerals have been used to identify the effects of open-system magmatic processes (*e.g.*, Gerlach & Grove 1982, Nixon & Pearce 1987, Kawamoto 1992, Stimac & Pearce 1992, Hauksdóttir 1994).

In this paper, we demonstrate the effects of assimilation on mineral zoning in plagioclase and pyroxene growing in an alkali olivine basaltic magma. Specifically, we explore the consequences of five simulations of magmatic assimilation on patterns of zoning in minerals using the MELTS program (Ghiorso & Sack 1995). The five simulations investigated include fractional crystallization (FC), fractional crystallization with concomitant assimilation (AFC) of bulk granite consisting of quartz (30% by volume), plagioclase (30%), K-feldspar (30%), and biotite (10%), and fractional crystallization coupled with assimilation of each mineral phase within the granite. For each simulation, we summarize the physicochemical effects of assimilation of specific minerals, including changes in liquidus and solidus temperatures, sequence of crystallization, mineral compositions and, central to this paper, patterns of zoning in the constituent minerals.

Our modeling suggests that 1) mineral zoning profiles can be sensitive indicators of open-system behavior, 2) these profiles can be used to identify different types of assimilation, and 3) the incorporation of both kinetic and thermodynamic constraints for chemical interaction between mineral growth and dissolution will provide distinctly new views on the origins of patterns of zoning in minerals associated with open chemical systems.

MODEL PATHS OF ASSIMILATION

Overview

Assimilation can drastically change the nature and evolution of the host magma. It can change liquidus and solidus temperatures (*e.g.*, Bowen 1922, Reiners *et al.* 1995), modify sequences of crystallization (*e.g.*, Ghiorso & Kelemen 1987, Reiners *et al.* 1995), or cause significant changes in host-magma compositions, especially in levels of trace elements and isotopes (Taylor 1980, DePaolo 1981, Myers *et al.* 1986, McBirney *et al.* 1987, Nielsen 1990, Grunder 1992, McCulloch *et al.* 1994, Luhr *et al.* 1995, Reiners *et al.* 1995). Consequently, for a given magma, assimilation can produce substantially different lines of descent of the liquid and different rock-types than fractional crystallization alone (*e.g.*, Kelemen & Ghiorso 1986, Nielsen 1988).

Two different styles of assimilation have been recognized and reported in the literature: *bulk assimilation* and *selective assimilation*. Bulk assimilation occurs where the material being assimilated by a given melt is added in proportions equal to the bulk xenolith's composition. Selective assimilation occurs where the composition of the assimilant added to the host melt is not equal to that of the bulk xenolith. The effects of both end-member processes have been recognized in natural magmatic systems (*e.g.*, Doe *et al.* 1969, Watson 1982, Kitchen 1989, Blichert-Toft *et al.* 1992, Philpotts & Asher 1993, Geist & White 1994, Reiners *et al.* 1995, Russell *et al.* 1995).

Ultimately, quantitative models combining thermodynamics, mass balance and kinetics are needed to model accurately the consequences of assimilation. Although such models are currently unavailable, many of the consequences of bulk and selective assimilation are adequately demonstrated by using existing models that combine equilibrium thermodynamics and mass balance (Nielsen 1988, Ghiorso & Sack 1995). Traditional petrological techniques for modeling both closed- and open-system behavior in magmas have recently been substantially improved by the revision of a thermodynamic database for silicate melts and the release of a computer program (MELTS). MELTS can simultaneously model igneous phase-equilibria relationships and mass-balance relationships for both open and closed systems (Ghiorso & Sack 1995).

TABLE 1. CHEMICAL AND MODAL COMPOSITION OF ALKALI OLIVINE BASALT SH-44[1] FROM LAVA FORK, NORTHWESTERN BRITISH COLUMBIA

Oxides	Wt. %	Minerals	Vol. %
SiO_2	46.46	Phenocrysts [Plagioclase, Olivine]	20
TiO_2	2.84		
Al_2O_3	16.92		
Fe_2O_3	2.59	Groundmass [Plagioclase, Olivine, Augite, Opaque phases]	55
FeO	10.10		
MnO	0.18		
MgO	6.52		
CaO	8.87	Vesicles	25
Na_2O	3.71		
K_2O	1.09		
P_2O_5	0.45		
H_2O	0.10		
Total	99.83		

[1]Hauksdóttir (1994)

TABLE 2. SUMMARY OF SEQUENCE OF CRYSTALLIZATION FOR EACH OF THE MODEL SIMULATIONS

Model Simulation[1]	Phase[2]	Saturation T (°C)[3]	Saturation Composition[4]	Composition Range	Total mass crystallized in g[5]
1	Pl	1175 (1035)	An_{71}	An_{71-3}	53.2
	Ol	1170 (1035)	Fo_{79}	Fo_{79-62}	9.2
	Spl	1125	Spl_{47}	Spl_{47-17}	13.5
	Cpx	1120	Di_{44}	Di_{43-49}	12.9
2	Pl	1170 (1045)	An_{70}	An_{70-26}	46.7 (38.9)
	Ol	1170 (1050)	Fo_{79}	Fo_{79-65}	10.2 (8.5)
	Spl	1125	Spl_{45}	Spl_{45-19}	14.0 (11.7)
	Cpx	1115	Di_{44}	Di_{43-52}	12.1 (10.0)
	Kfs	1045	$Ab_{48}An_9Or_{43}$	$Ab_{48}An_9Or_{43}$-$Ab_{47}An_3Or_{49}$	18.3 (15.3)
3	Pl	1170	An_{68}	An_{68-34}	45.1 (37.6)
	Ol	1170 (1120)	Fo_{79}	Fo_{79-70}	7.0 (5.9)
	Opx	1115 (1065)	En_{84}	En_{84-75}	11.9 (9.9)
	Spl	1110 (995)	Spl_{33}	Spl_{33-14}	9.0 (7.5)
	Pig	1060	Di_{25}	Di_{25-28}	5.7 (4.7)
	Rhom	990	Ilm_{83}	Ilm_{83}	0.2 (0.2)
4	Pl	1175 (1015)	An_{71}	An_{71-5}	68.2 (56.9)
	Ol	1170 (1120)	Fo_{80}	Fo_{80-60}	10.7 (8.9)
	Spl	1130	Spl_{50}	Spl_{50-17}	12.9 (10.8)
	Cpx	1110	Di_{44}	Di_{44-40}	8.1 (6.7)
5	Pl	1170 (1065)	An_{71}	An_{71-35}	36.7 (30.6)
	Ol	1170 (1065)	Fo_{79}	Fo_{79-67}	9.5 (7.9)
	Spl	1125 (1030)	Spl_{41}	Spl_{41-30}	13.0 (10.8)
	Cpx	1115	Di_{44}	Di_{43-49}	14.69 (12.2)
	Rhom	1025	Ilm_{73}	Ilm_{73-78}	0.4 (0.3)
	Kfs	1060	$Ab_{39}An_8Or_{52}$	$Ab_{39}An_8Or_{52}$-$Ab_{37}An_2Or_{61}$	36.3 (30.3)
6	Ol	1170 (1055)	Fo_{79}	Fo_{79-62}	13.2 (11.0)
	Pl	1160 (1055)	An_{71}	An_{71-32}	38.4 (32.0)
	Spl	1120	Spl_{38}	Spl_{38-14}	19.4 (16.2)
	Cpx	1115	Di_{44}	Di_{43-50}	14.5 (12.1)
	Kfs	1050	$Ab_{42}An_8Or_{50}$	$Ab_{42}An_8Or_{50}$-$Ab_{46}An_4Or_{50}$	22.1 (18.4)

[1] Simulations are defined as follows: 1: fractional crystallization of basaltic magma; 2: fractional crystallization coupled with assimilation of granite, 3: with Qtz, 4: with An_{10}, 5: with Ksp, and 6: with Phl_{30}

[2] All phases are solid solutions (e.g., Spl represents solid solution between chromite, hercynite, magnetite, spinel and ulvöspinel; Rhom represents solid solution between rhombohedral oxides including ilmenite, hematite, geikielite and pyrophanite)

[3] (- -) indicates temperature at which crystallization of phase stops

[4] Reported as mole fraction of selected endmember composition

[5] (- -) indicates percent of total system mass

Magmatic assimilation is one of the open-system processes that can be modeled with this new algorithm.

Using MELTS (Ghiorso & Sack 1995), we examined the consequences of bulk *versus* selective assimilation on the model path of fractional crystallization of an alkali olivine basaltic magma (Table 1). The starting composition of the magma is that of a basalt from Lava Fork, a Quaternary volcanic center in northwestern British Columbia (Hauksdóttir *et al.*

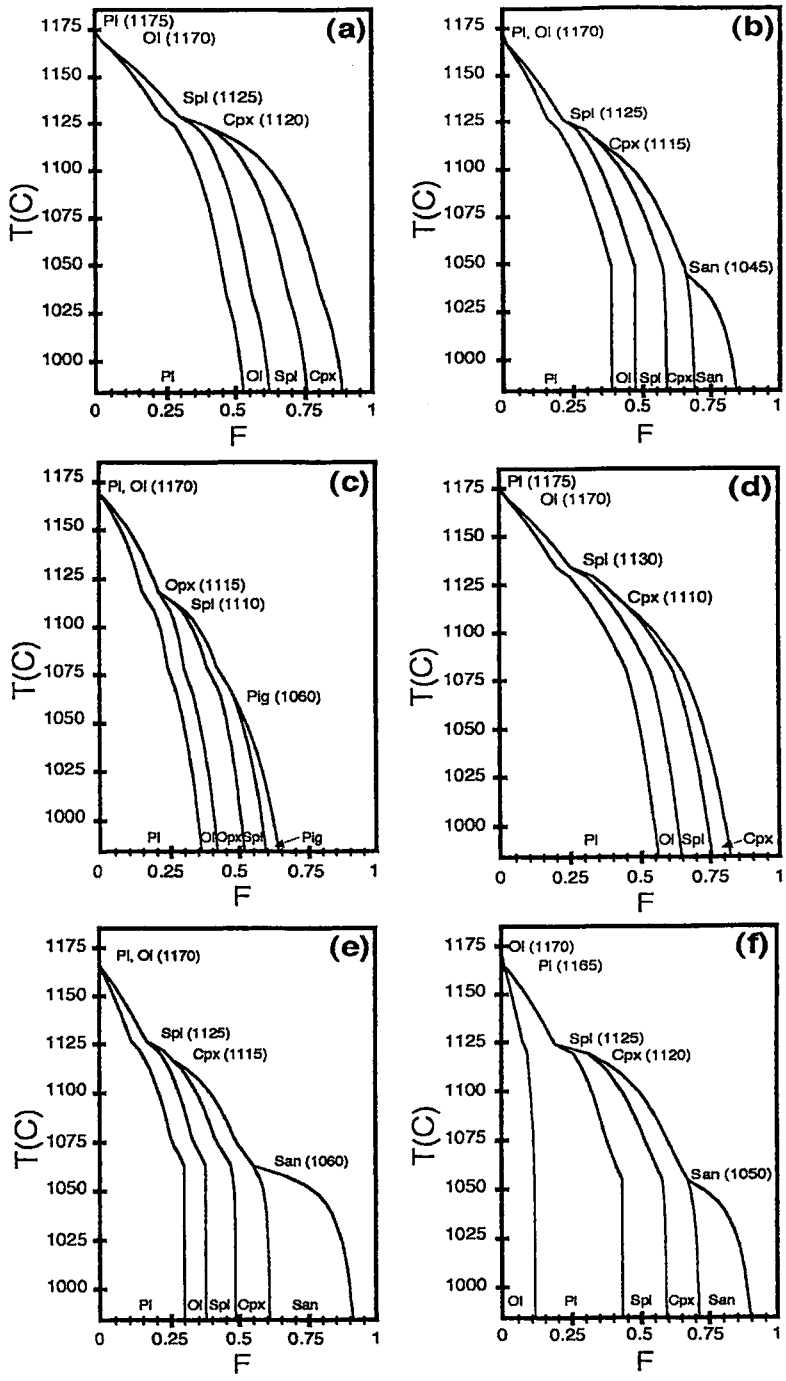

FIG. 1. Six model simulations are represented as F (fraction of system crystallized) *versus* magmatic T (°C) for: a) fractional crystallization (FC) of basaltic magma, and FC combined with assimilation (AFC) of b) granite, c) Qtz, d) Plagioclase (An_{10}); e) Ksp; and Bt (Phl_{30}). Saturation temperatures are shown for individual phases. Mineral abbreviations are from Kretz (1983).

1994, Hauksdóttir 1994). This sample was chosen because: a) it is chemically and petrographically well characterized, b) alkali olivine basalt is an important component of Quaternary magmatism in the northern Cordillera (Souther & Yorath 1991), and c) Hauksdóttir (1994) documented the importance of assimilation of granite in explaining the chemical variations within and among Quaternary lavas from this region.

The model fractionation paths are coupled to bulk assimilation of a typical granite (30% quartz, 30% plagioclase, 30% K-feldspar, 10% biotite) or to assimilation of the individual minerals within the granite. The latter models represent potential end-members of selective assimilation, which, on the basis of kinetic considerations for mineral dissolution in melts (see Discussion), are probably common in nature. For all simulations, pressure was fixed at 10^5 Pa, and $f(O_2)$, at the FMQ buffer. Assimilation simulations used a total of 20 g of assimilant as input into an initial mass of 100 g of magma; the assimilant was added in intervals of 1 g per temperature step for the first 20 temperature steps. The cooling interval for each of the simulations was 200°C, from 1185° to 985°C, using 5°C temperature steps.

The model simulations approximate conditions in a magmatic open system. Mass is added to the system by assimilation and removed by fractional crystallization. Heat is removed from the system *via* the imposed cooling rate of 5°C and the heat requirements of fusing 1 g of assimilant at each step. Previous investigators have outlined in detail the heat balances attending magmatic assimilation (*e.g.*, Nicholls & Stout 1982). The overall heat requirement for assimilation is dominated by two components: i) the energy required to bring the solid material from its initial temperature to the temperature of the magma, and ii) the energy to fuse the solid at the temperature of the magma (Nicholls & Stout 1982, Ghiorso & Kelemen 1987, Russell 1988, Russell *et al.* 1995). Investigators who have quantitatively explored the magnitude of the heating effect relative to the overall thermal budget for assimilation have found it to be a potentially significant effect on the amount of crystallization and cooling required by assimilation (*cf.* Ghiorso & Kelemen 1987, Reiners *et al.* 1995, Russell *et al.* 1995). Russell *et al.* (1995) showed explicitly (their Table 3, p. 11) the differences in the calculated heats of assimilation as a function of rock type and initial temperature. For all the model simulations discussed below, the initial temperature of the assimilant was 500°C.

Results of each simulation, including phase-saturation temperatures, saturation compositions, compositional ranges and total mass crystallized, are summarized in Table 2. Figure 1 (a to f) shows the calculated sequences of crystallization and cumulative phase proportions from each of the five assimilation simulations. Data for the case of FC alone (Fig. 1a) are shown in order to provide a contrast between the path of crystallization for the uncontaminated magma and the paths resulting from assimilation.

Results

The model FC path for the alkali olivine basalt SH–44 (Fig. 1a) has plagioclase as the liquidus phase (1175°C) followed closely by olivine (1170°C), spinel (1125°C) and clinopyroxene (1120°C). Plagioclase precipitates over the entire interval of crystallization, with a continuous variation in composition from An_{71} to An_4. The sequence of crystallization produced by MELTS parallels that established petrographically for SH–44 (Hauksdóttir 1994; Table 1).

The second simulation (Fig. 1b) models fractional crystallization and bulk assimilation of granite (AFC) consisting of 30% quartz, 30% plagioclase (An_{10}), 30% potassium feldspar and 10% biotite [Phl_{30}: $K_2Fe_{4.2}Mg_{1.8}Al_2Si_6O_{20}(OH)_4$]. The changes in sequence of crystallization and the predicted ranges in mineral compositions are surprisingly small, even though the total mass added to the system represents 20% by weight of the original magmatic system (Table 2). However, an important difference between this simulation and simulation 1 (FC only) is the abrupt appearance of sanidine as the equilibrium feldspar ($Ab_{48}An_9Or_{43}$) at 1045°C (Fig. 1b). Other differences arising from bulk assimilation of granite include coprecipitation of plagioclase and olivine as liquidus phases, 10 – 15°C changes in their crystallization intervals, and small differences in the composition of the crystallizing minerals [less than ~3 mol.% for olivine (Fo), spinel (Spl) and pyroxene (Di)]. Overall, with the exception of the appearance of sanidine, the two simulations produce similar results.

The last four simulations contrast the effects of selective assimilation of granite and its bulk assimilation (Figs. 1c to 1f; Table 2, simulations 3–6). Each of the four simulations uses 20 g of one of the phases in the bulk granite (Qtz, An_{10}, Ksp, Phl_{30}), with the same temperature and pressure conditions as in the first two simulations. Paths of selective assimilation are markedly different from both the FC and bulk-assimilation paths in crystallization sequence, the phases crystallized, proportions of cumulates produced and the range of mineral compositions. The only two factors that are relatively constant throughout all six simulations are the saturation compositions and temperatures for olivine and plagioclase (Table 2), as the initial composition of the magma is affected only slightly by assimilation in the first 15°C.

Fractional crystallization with assimilation of quartz produces a crystallization path that is markedly different from either of the first two simulations (Fig. 1c, Table 2). Plagioclase crystallizes throughout the simulation, yet has a relatively narrow range of compositions (An_{68} to An_{34}). Olivine has a shorter

crystallization interval (55°C) and is replaced by orthopyroxene at 1150°C, which is in turn replaced by pigeonite at 1060°C. Another minor change in the crystallization sequence is the late appearance of rhombohedral oxide (Ilm_{83}), replacing spinel in the crystallizing assemblage at 990°C.

The fourth simulation involves FC with assimilation of An_{10}. The crystallization path is again distinct from the previous simulations (Fig. 1d, Table 2). The most distinctive feature of the path pertains to plagioclase; it is the first phase to precipitate at 1175°C, and its total mass crystallized is almost 50% more than in any of the other assimilation simulations and 30% more than in the FC simulation. Similar to simulation 1, the composition of the plagioclase changes continuously from An_{71} to An_5, which is a broader range than for the Qtz assimilation simulation, yet without the abrupt appearance of sanidine as with bulk assimilation of granite.

The last two simulations both involve fractional crystallization with assimilation of a K-rich phase, either Ksp (Fig. 1e, Table 2, simulation 5) or Phl_{30} (Fig. 1f, Table 2, simulation 6). The important characteristics of both of these last two simulations are the abbreviated intervals of crystallization for An-rich plagioclase, the abrupt compositional change from plagioclase to sanidine at 1060°C for simulation 5 and at 1050°C for simulation 6 ($Ab_{52}An_{35}Or_{13}$ to $Ab_{39}An_8Or_{52}$ and $Ab_{54}An_{32}Or_{14}$ to $Ab_{42}An_8Or_{50}$, respectively) and the large total mass of sanidine crystallized (Table 2). Simulation 5 produces a small amount of rhombohedral oxide, and in simulation 6, olivine replaces plagioclase as the liquidus phase at 1170°C.

Assimilation and Mineral Zoning

As pointed out by Bowen (1922) and more recent investigators (Wilcox 1954, Kushiro 1975, Nicholls & Stout 1982, Kelemen & Ghiorso 1986, Ghiorso & Kelemen 1987, Nielsen 1988, Reiners *et al.* 1995, Russell *et al.* 1995), one of the important consequences of assimilation is to change the crystallization interval of individual phases as well as of the magma as a whole. Three of the AFC simulations (granite, Qtz, An_{10}) effectively extend the crystallization interval for SH–44 beyond what is predicted for the pure FC path. In contrast, AFC of either of the K-rich minerals (Ksp and Phl_{30}) slightly shortens the interval of magmatic crystallization (Fig. 1).

The AFC paths simulated above also produce significant differences in the range of mineral compositions produced during crystallization (*e.g.*, Fig. 2). Variations in mineral compositions for plagioclase

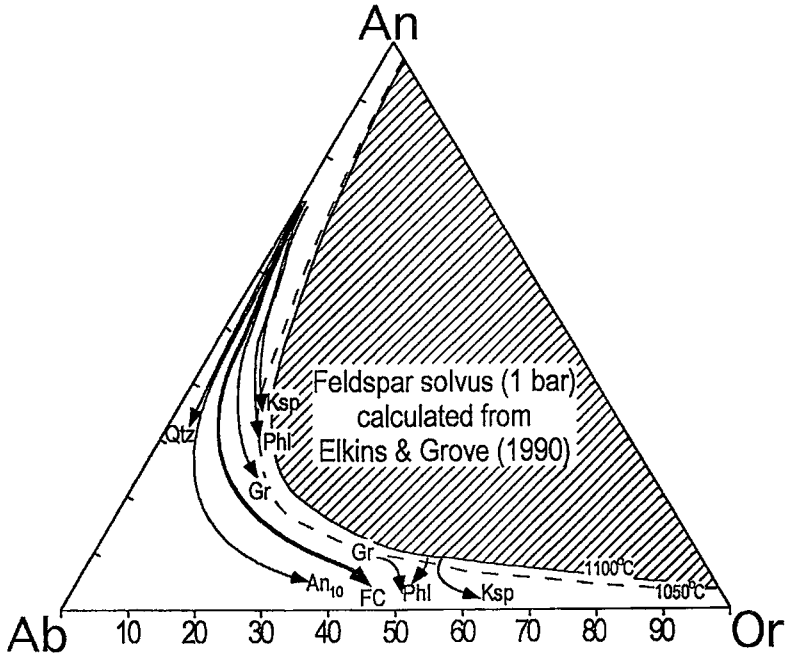

FIG. 2. Ternary feldspar diagram showing distribution of model feldspar compositions derived from six model simulations (lines with arrows), including FC, and AFC of granite (Gr), Qtz, An_{10}, Ksp and Phl_{30}. Projected feldspar solvus is for 1 bar and 1100° (solid) and 1050°C (dashed) (calculated from Elkins & Grove 1990).

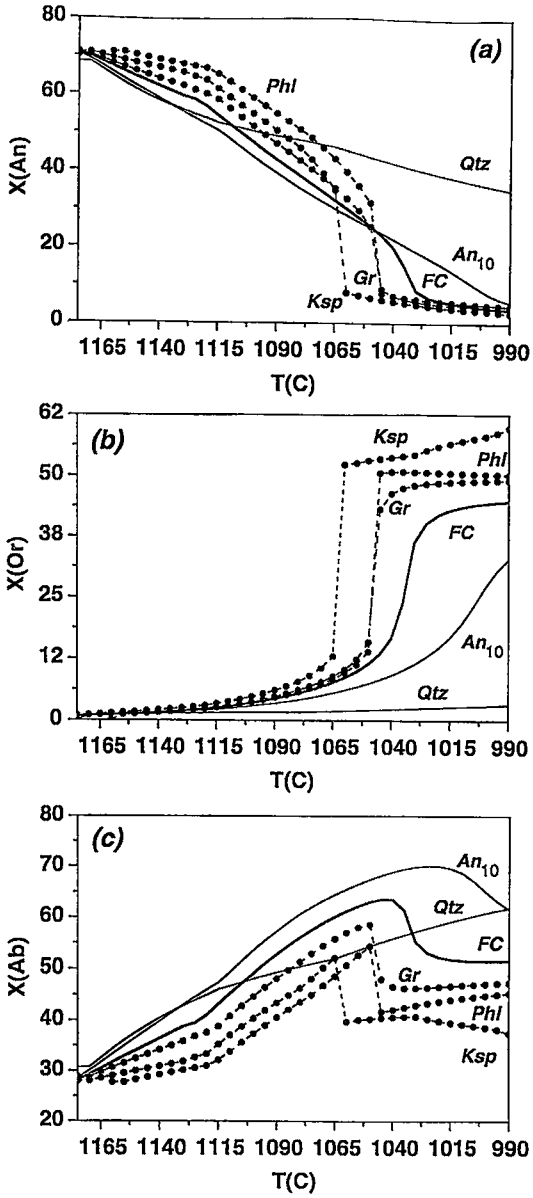

FIG. 3. Model feldspar compositions, in terms of a) X_{An}, b) X_{Or} and c) X_{Ab}, are plotted against T (°C). Labels for the six simulations are as in Figure 2.

(Fig. 3) and pyroxene (Fig. 4) have been summarized as a function of temperature, and crudely represent expected compositional profiles for crystals growing continuously in the melt without intercrystalline diffusional re-equilibration.

Feldspar

Plagioclase is an important product of crystallization in this basaltic system at P = 10^5 Pa because it is the liquidus phase in five of the six simulations and crystallizes over more than 50% of the crystallization interval for every simulation. Consequently, its composition records the chemical path taken by the magma during crystallization and assimilation. The feldspar compositions for each of the simulations are shown in Figure 2. The six simulations produce three different patterns of zoning. The first, demonstrated by the Qtz assimilation simulation, has very little curvature, *i.e.* with decreasing X_{An} and increasing X_{Ab}, there is little to no change in X_{Or}. This path also has a relatively narrow range in X_{An}. The second path, that of both the FC and the An_{10} assimilation simulations, follows a continuous curve of decreasing X_{An} and increasing X_{Ab} and X_{Or}. The third pattern, generated by the other three simulations (bulk granite, Ksp, Phl_{30}), is discontinuous.

Predicted patterns of composition for An, Or and Ab in feldspar in each of the simulations are shown in Figure 3. The zoning profiles produced by the bulk granite, Ksp and Phl_{30} assimilation paths are similar in shape to the FC path except that at 1045°, 1060° and 1050°C, respectively, sanidine replaces plagioclase as a crystallizing phase. However, the zoning paths for these three simulations predict An-rich, Or-rich and Ab-poor compositions relative to the FC path. As a consequence, the rim of plagioclase crystals produced by these three assimilation simulations would be expected to be much more An-rich than the rim of plagioclase produced by fractional crystallization. Each of the three assimilation simulations produce paths that could ultimately lead to the formation of an antirapakivi texture in the rock (sanidine mantles on plagioclase).

Both the Qtz and the An_{10} assimilation simulations produce zoning paths that contrast sharply with the FC path (Fig. 3). For the Qtz AFC path, plagioclase precipitates throughout the entire interval of crystallization, and K-feldspar does not crystallize at all. The Qtz path also produces a more uniform zoning profile in plagioclase from the core to the rim. The An_{10} path also has a strong buffering effect on the zoning profile and is quite similar in shape to the FC profile (Fig. 2). At the low-T end of the crystallization interval, Ab decreases and Or increases for both the An_{10} and FC simulations. However, unlike the FC simulation, the An_{10} simulation does not have a flat compositional profile for all three feldspar components at low temperatures. And unlike the granite, Ksp and Phl_{30} simulations, the compositional shift to Or-rich feldspar for the An_{10} simulation is gradual and occurs in the last 30°C in the crystallization interval. Thus, the ternary feldspar solvus is never intersected.

The simulated zoning profiles (Fig. 3) have both

obvious and somewhat unexpected characteristics. Bowen (1922) demonstrated that assimilation of plagioclase with a higher X_{Ab} content than the equilibrium feldspar composition extends the total interval of crystallization of plagioclase. Similarly, adding quartz to this alkaline basalt destabilizes clinopyroxene, resulting in a more An-rich plagioclase. Also it seems intuitive that adding components rich in K to the system would stabilize sanidine. What is somewhat unexpected is that adding components rich in K early in the crystallization interval produces a plagioclase "core" with a relatively more An-rich composition than for FC alone. The "rim" of plagioclase phenocrysts produced in the Ksp and Phl_{30} simulations have a lower X_{Or} than for the FC or An_{10} simulations. Overall, the important point illustrated by these patterns is that they are highly dependent on the nature of contamination, either bulk or selective, and extent of assimilation. Such patterns should be recognizable in natural samples.

Pyroxene

Clinopyroxene crystallization is predicted for the FC simulation and four of the five AFC simulations; the Qtz simulation predicts only clinoenstatite (1115°C) and pigeonite (1060°C) crystallization. As with feldspar, changes in mineral composition of the pyroxenes are sensitive recorders of the different model paths of assimilation (Fig. 4). In all cases, the X_{Di} component in pyroxene initially decreases slightly. However, for the granite, Ksp and Phl_{30} simulations, the X_{Di} component begins to increase steeply at the point where sanidine begins to crystallize. For the Ksp assimilation path, at 1060°C, the X_{Di} component shows a distinctive, sharp increase, followed by a more gradual decrease to values less than the FC, granite or Phl_{30} simulations. The An_{10} path maintains a relatively constant value of X_{Di}.

The clinoenstatite component (X_{cEn}) has a pattern distinctly different from that of the X_{Di} component. It first increases with clinopyroxene crystallization then decreases, for all simulations. The change from increasing to decreasing X_{cEn} occurs again at the onset of sanidine crystallization for the Ksp, Phl_{30} and granite-assimilation simulations. The FC and An_{10} paths show much less variation in X_{cEn}.

The jadeite component (X_{Jd}) increases with decreasing temperature for all six of the simulations. The only major variation occurs for the Ksp, Phl_{30} and granite-assimilation simulations, where the onset of sanidine crystallization produces overall variations of more than 50% (0.02 X_{Jd}).

As with plagioclase, the assimilation paths initially produce pyroxenes with similar compositions to the case of fractional crystallization alone, with the exception of the Qtz assimilation simulation. However, as crystallization-assimilation proceeds, the compositional paths of the pyroxenes become more distinct. The addition of K appears to have the most distinctive effect on implied profiles of pyroxene crystals, as reflected in large variations in both X_{Di} and X_{Jd} components between the different paths. This is consistent with the experimental results of Kushiro (1975), who demonstrated that in synthetic silicate melt systems, the addition of K caused drastic shifts in cotectic boundaries.

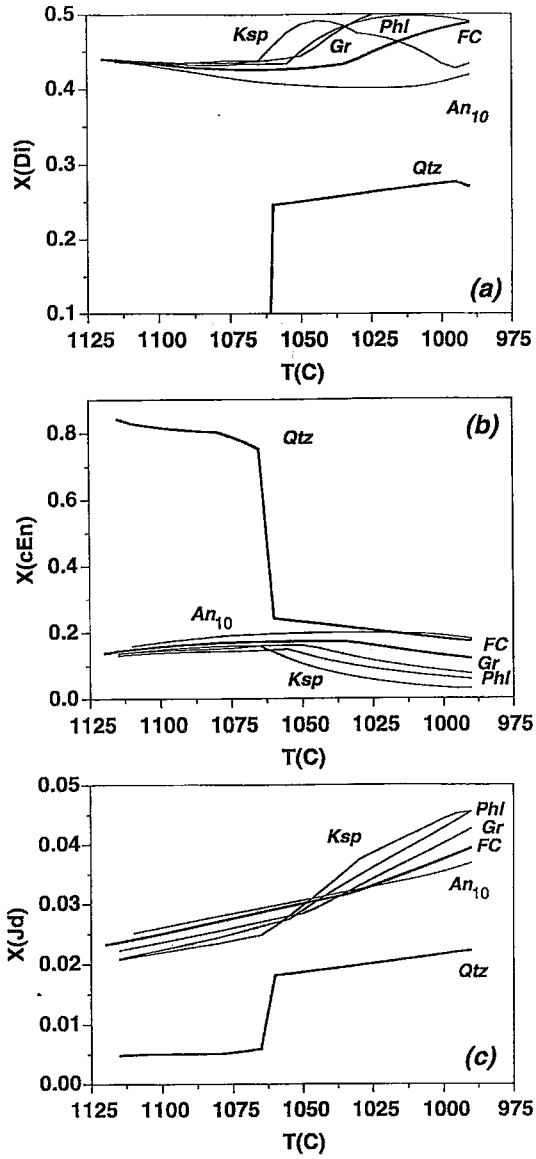

FIG. 4. Model pyroxene compositions, in terms of a) X_{Di}, b) X_{cEn} and c) X_{Jd} are plotted against T(°C). Labels as in Figures 2 and 3.

Models for chemical zoning in open systems

The equilibrium models presented above are an important first step toward understanding the linkages between patterns of mineral zoning and different types of magmatic assimilation. As a second step, we have developed a model for predicting rates of mineral dissolution in basaltic magma using the calculated thermodynamic potential affinity (Fig. 5; Edwards & Russell 1996). On the basis of our model at the liquidus temperature for simulation 2 (1175°C), the calculated rate of dissolution at which minerals in the granite will dissolve decreases in the following order: biotite, K-feldspar, plagioclase, and quartz. Table 3 shows the calculated rates of mineral dissolution as well as the total time required to dissolve 1-cm spheres of quartz, K-feldspar, plagioclase and biotite. This predicted order of mineral dissolution is consistent with observations on partly melted granitic xenoliths found in basaltic magmas, that the hydrous phases react faster than quartz, plagioclase or K-feldspar (*e.g.*, Larsen & Switzer 1939, Watson & Mathews 1948, Al-Rawi & Carmichael 1967, Kaczor *et al.* 1988, Hauksdóttir 1994).

We can also model the production of melt as well as the changing composition of the melt from the granite used in the AFC simulation as a function of time (Table 4). For the granite, the first melts to be produced will be very K-rich, as biotite and K-feldspar both dissolve in the first two hours. The plagioclase continues to dissolve for an additional four hours, whereas quartz requires 33 hours to assimilate completely. We have not yet quantitatively modeled the expected patterns of zoning resulting from selective assimilation; however, the implications for plagioclase crystallization over this 33-hour period are clear. On the basis of the calculated order of mineral dissolution and the assimilation simulations presented above, we would expect 1) formation of an An-rich core with a higher X_{Or} than predicted for FC only owing to the rapid initial influx of K, 2) a steady decrease in X_{Or} and concomitant increase in X_{Ab} as K input ceases and Na continues to be added, and finally 3), as Si becomes the only component being added to the magma, the X_{An} might again increase if clinopyroxene is replaced by clinoenstatite, generating reversed zoning in the crystal near the rim. This speculation concerning the pattern of zoning in plagioclase hints at the possible complexities generated by selective assimilation.

Discussion

Mineral zoning and AFC

As demonstrated above (Figs. 1–4), each AFC simulation generates a distinct chemical–mineralogical path. Patterns of zoning in plagioclase and pyroxene and the proportions of phases crystallized are particularly sensitive recorders of these different paths. For example, in the Qtz assimilation simulation, both the plagioclase compositions (Fig. 3) and the proportions of phases crystallized (Table 2) are very different from those generated by the FC simulation. On the basis of these observations, patterns of mineral growth and zoning seem a promising way to recognize open-system behavior and, possibly, to identify the type of assimilation (*e.g.*, bulk *versus* selective) responsible for the patterns.

Recently, Kitchen (1989) and Philpotts & Asher (1993) have attributed distinct patterns of chemical zoning found in magmatic minerals of mafic dykes to assimilation. Kitchen (1989) found that assimilation of granitic wallrock by clinopyroxene-bearing dolerite dykes caused both pigeonite and orthopyroxene to

TABLE 3. CALCULATED VALUES OF **A** AND **v** FOR MINERALS IN GRANITE AT 1175 °C AND 10^5 Pa[1]

Mineral	**A** (J mole^{-1})[2]	**v**• 10^{-7} (oxygen equiv. moles cm^{-2} s^{-1})[3]	Time to dissolve 1 cm sphere
Qtz	10,231	1.13	4.5 days
An_{10}	9,205	4.62	0.95 days
Ksp	25,879	13.37	7 hours
Phl_{30}	139,473	100.43	1 hour

[1] Model line used to calculate mineral dissolution rates (**v**) is **v** = 6.56 E-5 **A** - 0.213; values of **A** and **v** vary as a function of T and P

[2] **A** is the thermodynamic potential affinity and for chemical reactions at a specific T and P is equal to the sum of the chemical potentials of the reactants multiplied by their stoichiometric coefficients minus the sum of the chemical potentials of the products multiplied by their stoichiometric coefficients

[3] **v** is the predicted rate of mineral dissolution at a given T and P

TABLE 4. MODEL PREDICTION OF TIME REQUIRED TO INCORPORATE GRANITE BY SELECTIVE ASSIMILATION

Time	% Qtz	% Pl	% Ksp	% Phl	% Granite
1 hour	3	14	45	100	28.6
2 hours	6	29	89	100	47.2
1 day	74	100	100	100	82.2
100% dissolution (hours)	33	6.9	2.2	0.11	33

crystallize, and produced diverse patterns of compositional zoning in pyroxene. Kitchen (1989) also found enrichments of Na and K in the rim of large grains of plagioclase and in skeletal feldspars that were due to contamination. Philpotts & Asher (1993) reported that sections of oscillatory zoning in plagioclase phenocrysts in a contaminated diabase dyke consistently showed an "orthoclase spike" which, along with elevated X_{Or} in the core of the phenocrysts, was attributed to assimilation.

However, it is important to note that the physicochemical effects of assimilation need not be recorded in all phenocrysts of the contaminated magma. One of the trademarks of mineral growth and zoning studies is the large amount of variation seen in zoning and growth features within any one population of minerals (Wiebe 1968, Pringle *et al.* 1974, Kitchen 1989, Stimac & Wark 1992, Philpotts & Asher 1993, Hauksdóttir 1994). Many investigators (*e.g.*, Pringle *et al.* 1974, Sibley *et al.* 1976, Pearce & Kolisnik 1990, Pearce 1994) have suggested that growth features and compositional zoning in minerals record both local and global conditions in the magma. Minerals crystallizing and growing immediately adjacent to the xenoliths are most likely to record the chemical changes caused by assimilation.

Types of assimilation

An important question for those trying to recognize assimilation processes in magmatic systems is whether the type of contamination was bulk or selective. Several lines of evidence are consistent with the proposal that selective assimilation is dominant over bulk assimilation in natural systems; these include measurements of mineral-dissolution rates (Watson 1982; *cf.* Edwards & Russell 1996), the presence of isolated xenocrysts in host magmas (Wilcox 1954, Sato 1975, Kitchen 1989, Blichert-Toft *et al.* 1992, Luhr *et al.* 1995, among others), and the composition of glass in partly melted xenoliths (LeMaitre 1974, Philpotts & Asher 1993, Hauksdóttir 1994, among others). In particular, experimentally observed rates of dissolution suggest that the mineral phases in xenoliths do not react with the host magma at the same rate (Fig. 5, inset).

The consequences of misidentifying bulk *versus* selective assimilation can be severe in modeling the chemical evolution of open magmatic systems. For example, trace element or isotope mass-balance calculations based on the assumption of bulk assimilation may drastically overestimate the amount of actual contamination. One of the most important parameters used for such mass-balance models is the ratio of assimilation to crystallization (DePaolo 1981). Reiners *et al.* (1995) demonstrated that this ratio is highly dependent on the composition of the material being assimilated, and that the isotopic differences resulting from bulk assimilation of pelite *versus* the assimilation of a partial melt of the pelite are significant. Figures 3 and 4 show that selective assimilation of the individual phases in a granite xenolith produces distinctly different patterns of zoning than does bulk assimilation of granite. Thus, as demonstrated above, compositional zoning in minerals could provide an alternative means for identifying the extent and chemical pathways of assimilation.

Conclusions

Patterns of mineral zoning preserve records of the chemical pathways taken by the host magma during crystallization. We have demonstrated, using an existing equilibrium thermodynamic model, that bulk and selective assimilation produce distinct, recognizable patterns of mineral growth and zoning.

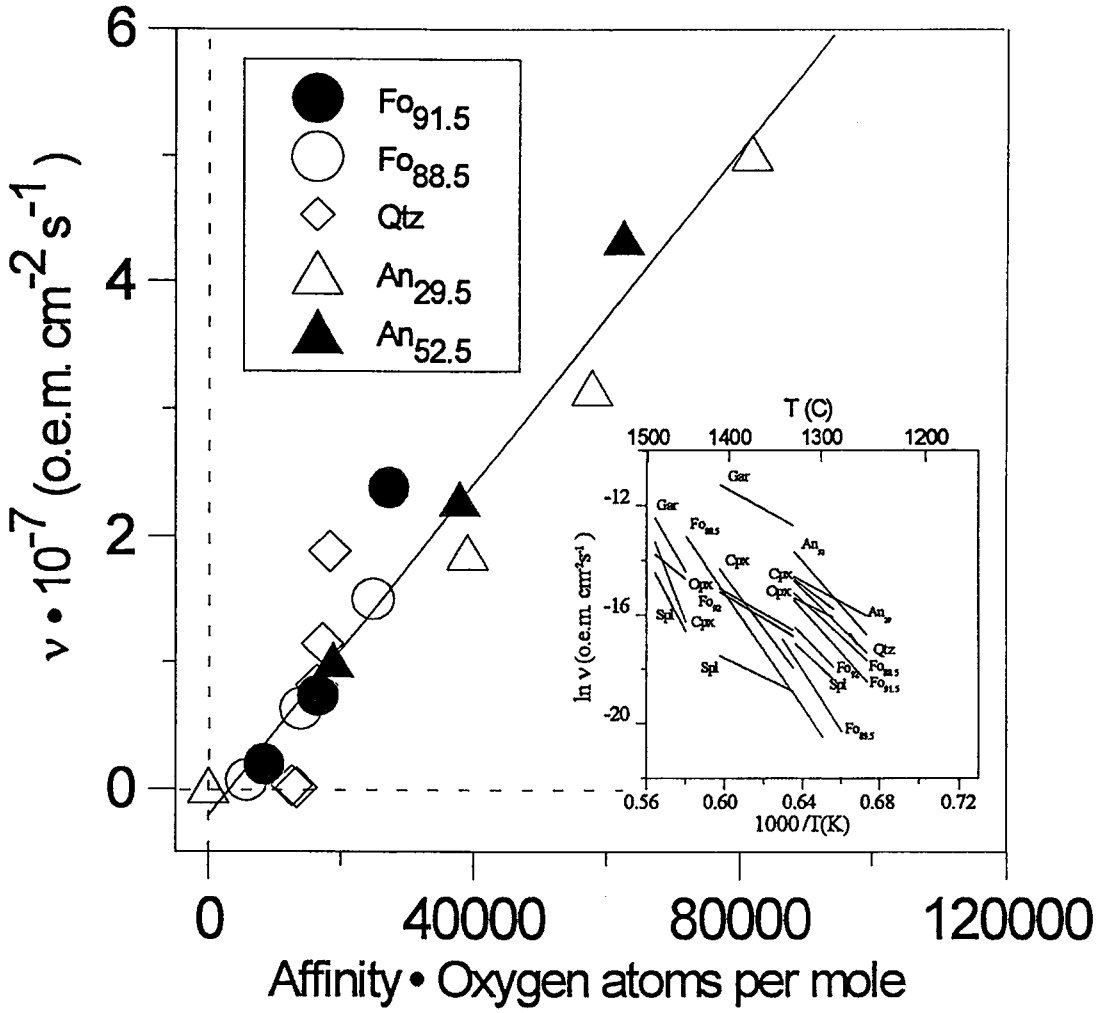

FIG. 5. Diagram of υ (oxygen equivalent moles cm^{-2} s^{-1}) *versus* A (J • number of oxygen atoms $mole^{-1}$ of mineral) for Qtz, Plagioclase and Ol derived from 1-atmosphere mineral-dissolution experiments of Donaldson (1985). Values of A were calculated using the MELTS software (Ghiorso & Sack 1995; http://msgmac.geology.washington.edu/MeltsWWW/Melts.html). Inset shows ln υ *versus* 1/T (K) for a variety of minerals in basaltic magmas (Edwards & Russell 1996).

We believe that patterns of compositional zoning in minerals can be used to better constrain hypotheses dealing with open- *versus* closed-system behavior. Estimates of amounts of contamination may then be calculated from trace-element concentrations or isotopic ratios if the contaminant can be characterized. We are working to build an integrated kinetic and thermodynamic model to simulate the complexity inherent in open-system magmatic processes: patterns of zoning in minerals represent rigid constraints on these processes.

ACKNOWLEDGEMENTS

Financial support for this research derives from a University Graduate Fellowship (UBC) to BRE and NSERC (OGP0820) and a LITHOPROBE grant to JKR. We thank G.M. Dipple, R.F. Martin, R. Mason, J. Nicholls, R. Nielsen and J.F.H. Thompson for critical reviews of the manuscript. Further information on modeling rates of mineral dissolution can be found on the WWW at http://perseus.geology.ubc.ca/~bedwards/index/html. This is LITHOPROBE contribution 763.

REFERENCES

AL-RAWI, Y. & CARMICHAEL, I.S.E. (1967): A note on the natural fusion of granite. *Am. Mineral.* **52**, 1806-1814.

ANDERSON, A.T., JR. (1984): Probable relations between plagioclase zoning and magma dynamics, Fuego volcano, Guatemala. *Am. Mineral.* **69**, 660-676.

BLICHERT-TOFT, J., LESHER, C.E. & ROSING, M.T. (1992): Selectively contaminated magmas of the Tertiary East Greenland macrodike complex. *Contrib. Mineral. Petrol.* **110**, 154-172.

BOWEN, N.L. (1922): The behavior of inclusions in igneous magmas. *J. Geol.* **30**, 513-570.

CLARK, A.H., PEARCE, T.H., ROEDER, P.L. & WOLFSON, I. (1986): Oscillatory zoning and other microstructures in magmatic olivine and augite: Nomarski interference contrast observations on etched polished surfaces. *Am. Mineral.* **71**, 734-741.

DEPAOLO, D.J. (1981): Trace element and isotopic effects of combined wallrock assimilation and fractional crystallization. *Earth Planet. Sci. Lett.* **53**, 189-202.

DOE, B.R., LIPMAN, P.W., HEDGE, C.E. & KURASAWA, H. (1969): Primitive and contaminated basalts from the southern Rocky Mountains, U.S.A. *Contrib. Mineral. Petrol.* **21**, 142-156.

DONALDSON, C.H. (1985): The rates of dissolution of olivine, plagioclase and quartz in a basalt melt. *Mineral. Mag.* **49**, 683-693.

EDWARDS, B.R. & RUSSELL, J.K. (1996): A review and analysis of mineral dissolution rates in naturally occurring silicate melts. *Chem. Geol.* **130**, 233-245.

ELKINS, L.T. & GROVE, T.L. (1990): Ternary feldspar experiments and thermodynamic models. *Am. Mineral.* **75**, 544-559.

GEIST, D. & WHITE, C. (1994): Assimilation and fractionation in adjacent parts of the same magma chamber: Vandfaldsdalen macrodike, East Greenland. *Contrib. Mineral. Petrol.* **116**, 92-107.

GERLACH, D.C. & GROVE, T.L. (1982): Petrology of Medicine Lake Highland volcanics: characterization of endmembers of magma mixing. *Contrib. Mineral. Petrol.* **80**, 147-159.

GHIORSO, M.S. & KELEMEN, P.B. (1987): Evaluating reaction stoichiometry in magmatic systems evolving under generalized thermodynamic constraints: examples comparing isothermal and isenthalpic assimilation. *In* Magmatic Processes: Physicochemical Principles (B.O. Mysen, ed.). *The Geochemical Society, Spec. Publ.* **1**, 319-336.

_____ & SACK, R.O. (1995): Chemical mass transfer in magmatic processes. IV. A revised and internally consistent thermodynamic model for the interpolation and extrapolation of liquid-solid equilibria in magmatic systems at elevated temperatures and pressures. *Contrib. Mineral. Petrol.* **119**, 197-212.

GRUNDER, A.L. (1992): Two-stage contamination during crustal assimilation: isotopic evidence from volcanic rocks in eastern Nevada. *Contrib. Mineral. Petrol.* **112**, 219-229.

HAUKSDÓTTIR, S. (1994): *Petrography, Geochemistry and Petrogenesis of the Iskut – Unuk Rivers Volcanic Centres, Northwestern British Columbia.* M.Sc. thesis, Univ. of British Columbia, Vancouver, British Columbia.

_____, ENEGREN, E.G. & RUSSELL, J.K. (1994): Recent basaltic volcanism in the Iskut – Unuk rivers area, northwestern British Columbia. *Geol. Soc. Can., Current Res.* **1994-A**, 57-67.

JAMTVEIT, B. (1991): Oscillatory zonation patterns in hydrothermal grossular-andradite garnet: nonlinear dynamics in regions of immiscibility. *Am. Mineral.* **76**, 1319-1327.

KACZOR, S.M., HANSON, G.N. & PETERMAN, Z.E. (1988): Disequilibrium melting of granite at the contact with a basic plug: a geochemical and petrographic study. *J. Geol.* **96**, 61-78.

KAWAMOTO, T. (1992): Dusty and honeycomb plagioclase: indicators of processes in the Uchino stratified magma chamber, Izu Peninsula, Japan. *J. Volc. Geotherm. Res.* **49**, 191-208.

KELEMEN, P.B. & GHIORSO, M.S. (1986): Assimilation of peridotite in zoned calc-alkaline plutonic complexes: evidence from the Big Jim complex, Washington Cascades. *Contrib. Mineral. Petrol.* **94**, 12-28.

KITCHEN, D.E. (1989): The disequilibrium partial melting and assimilation of Caledonian granite by Tertiary basalt at Barnesmore, Co. Donegal. *Geol. Mag.* **126**, 397-405.

KRETZ, R. (1983): Symbols for rock-forming minerals. *Am. Mineral.* **68**, 277-279.

KUO, LUNG-CHUAN & KIRKPATRICK, R.J. (1982): Pre-eruption history of phyric basalts from DSDP legs 45 and 46: evidence from morphology and zoning patterns in plagioclase. *Contrib. Mineral. Petrol.* **79**, 13-27.

KUSHIRO, I. (1975): On the nature of silicate melt and its significance in magma genesis: regularities in the shift of the liquidus boundaries involving olivine, pyroxene, and silica minerals. *Am. J. Sci.* **275**, 411-431.

LARSEN, E.S. & SWITZER, G. (1939): An obsidian-like rock formed from the melting of a granodiorite. *Am. J. Sci.* **237**, 562-568.

LEMAITRE, R.W. (1974): Partially fused granite blocks from Mt. Elephant, Victoria, Australia. *J. Petrol.* **15**, 403-412.

LUHR, J.F., PIER, J.G., ARANDA-GÓMEZ, J.J. & PODOSEK, F.A. (1995): Crustal contamination in early Basin-and-Range hawaiites of the Los Encinos Volcanic Field, central México. *Contrib. Mineral. Petrol.* **118**, 321-339.

MCBIRNEY, A.R., TAYLOR, H.P. & ARMSTRONG, R.L. (1987): Paricutin re-examined: a classic example of crustal assimilation in calc-alkaline magma. *Contrib. Mineral. Petrol.* **95**, 4-20.

MCCULLOCH, M.T., KYSER, T.K., WOODHEAD, J.D. & KINSLEY, L. (1994): Pb–Sr–Nd–O isotopic constraints on the origin of rhyolites from the Taupo Volcanic Zone of New Zealand: evidence of assimilation followed by fractionation from basalt. *Contrib. Mineral. Petrol.* **115**, 303-312.

MYERS, J.D., FROST, C.D. & ANGEVINE, C.L. (1986): A test of a quartz eclogite source for parental Aleutian magmas: a mass balance approach. *J. Geol.* **94**, 811-828.

NEKVASIL, H. (1994): Ternary feldspar/melt equilibria: a review. *In* Feldspars and their Reactions (I. Parsons, ed.). Kluwer Academic Publ., Dordrecht, The Netherlands (195-219).

NICHOLLS, J. & STOUT, M.Z. (1982): Heat effects of assimilation, crystallization and vesiculation in magmas. *Contrib. Mineral. Petrol.* **81**, 328-339.

NIELSEN, R.L. (1988): A model for the simulation of combined major and trace element liquid lines of descent. *Geochim. Cosmochim. Acta* **52**, 27-38.

_____ (1990): Phase equilibria constraints on liquid lines of descent generated by paired assimilation and fractional crystallization: trace elements and Sr and Nd isotopes. *J. Geophys. Res.* **94**, 787-794.

NIXON, G.T. & PEARCE, T.H. (1987): Laser-interferometry study of oscillatory zoning in plagioclase: the record of magma mixing and phenocryst recycling in calc-alkaline magma chambers, Iztaccíhuatl Volcano, Mexico. *Am. Mineral.* **72**, 1144-1162.

PEARCE, T.H. (1994): Recent work on oscillatory zoning in plagioclase. *In* Feldspars and their Reactions (I. Parsons, ed.). Kluwer Academic Publ., Dordrecht, The Netherlands (313-349).

_____, GRIFFIN, M.P. & KOLISNIK, A.M. (1987a): Magmatic crystal stratigraphy and constraints on magma chamber dynamics: Laser interference results on individual phenocrysts. *J. Geophys. Res.* **92**, 13,745-13,752.

_____ & KOLISNIK, A.M. (1990): Observations of plagioclase zoning using interference imaging. *Earth Sci. Rev.* **29**, 9-26.

_____, RUSSELL, J.K. & WOLFSON, I. (1987b): Laser-interference and Nomarski interference imaging of zoning profiles in plagioclase phenocrysts from the May 18, 1980 eruption of Mount St. Helens, Washington. *Am. Mineral.* **72**, 1131-1143.

PHILPOTTS, A.R. & ASHER, P.M. (1993): Wallrock melting and reaction effects along the Higganum diabase dike in Connecticut: contamination of a continental flood basalt feeder. *J. Petrol.* **34**, 1029-1058.

PRINGLE, G.J., TREMBATH, L.T. & PAJARI, G.E. (1974): Crystallization history of a zoned plagioclase. *Mineral. Mag.* **39**, 867-877.

REINERS, P.W., NELSON, B.K. & GHIORSO, M.S. (1995): Assimilation of felsic crust by basaltic magma: thermal limits and extents of crustal contamination of mantle-derived magmas. *Geology* **23**, 563-566.

RUSSELL, J.K. (1988): Aspects of heat transfer in magmas. *In* Heat, Metamorphism and Tectonics (E.G. Nisbet & C.M.R. Fowler, eds.). *Mineral. Assoc. Can., Short-Course Handbook* **14**, 117-154.

_____, EDWARDS, B.R. & SNYDER, L.D. (1995): Volatile production possibilities during magmatic assimilation: heat and mass-balance constraints. *In* Magmas, Fluids and Ore Deposits (J.F.H. Thompson, ed.). *Mineral. Assoc. Can., Short-Course Handbook* **23**, 1-24.

_____, NIXON, G.T. & PEARCE, T.H. (1987): Petrographic constraints on modelling the crystallization of basalt magma, Cow Lakes, southeast Oregon. *Can. J. Earth Sci.* **25**, 486-494.

SATO, H. (1975): Diffusion coronas around quartz xenocrysts in andesite and basalt from Tertiary volcanic region in northeastern Shikoku, Japan. *Contrib. Mineral. Petrol.* **50**, 49-64.

SIBLEY, D.F., VOGEL, T.A., WALKER, B.M. & BYERLY, G. (1976): The origin of oscillatory zoning in plagioclase: a diffusion and growth controlled model. *Am. J. Sci.* **276**, 275-284.

SOUTHER, J.G. & YORATH, C.J. (1991): Neogene assemblages. *In* Geology of the Cordilleran Orogen in Canada (H. Gabrielse & C.J. Yorath, eds.). *Geol. Surv. Can., Geology of Canada* **4**, 373-401.

STIMAC, J.A. & PEARCE, T.H. (1992): Textural evidence of mafic-felsic magma interaction in dacite lavas, Clear Lake, California. *Am. Mineral.* **77**, 795-809.

_____ & WARK, D.A. (1992): Plagioclase mantles on sanidine in silicic lavas, Clear Lake, California: implications for the origin of rapakivi texture. *Geol. Soc. Am., Bull.* **104**, 728-744.

TAYLOR, H.P., JR. (1980): The effects of assimilating country rock by magmas on the $^{18}O/^{16}O$ and $^{87}Sr/^{86}Sr$ systematics in igneous rocks. *Earth Planet. Sci. Lett.* **47**, 243-254.

UEBEL, P.J. (1978): The zoning of plagioclases as record of petrogenetic development of the Ben Nevis ring-intrusion, Scotland. *Neues Jahrb. Mineral., Abh.* **132**, 182-213.

WATSON, E.B. (1982): Basalt contamination by continental crust: some experiments and models. *Contrib. Mineral. Petrol.* **80**, 73-87.

WATSON, K. DE P. & MATHEWS, W.H. (1948): Partly vitrified xenoliths in pillow basalt. *Am. J. Sci.* **246**, 601-614.

WIEBE, R.A. (1968): Plagioclase stratigraphy: a record of magmatic conditions and events in a granite stock. *Am. J. Sci.* **266**, 690-703.

WILCOX, R.E. (1954): Petrology of the Parícutin volcano. *U.S. Geol. Surv., Bull.* **965-C**, 281-353.

Received January 10, 1996, revised manuscript accepted May 6, 1996.